

PACS numbers: 42.55.Ks; 82.30.Fi
DOI: 10.1070/QE2010v040n09ABEH014368

Kinetics of $O_2(^1\Delta)$ self-quenching in the $O_2-O_2(^1\Delta)-H_2O$ gas mixture

M.V. Zagidullin, N.A. Khvatov

Abstract. **The self-quenching kinetics of $O_2(^1\Delta)$ molecules in the $O_2-O_2(^1\Delta)-H_2O$ gas mixture produced by a chemical singlet-oxygen generator for an oxygen–iodine laser is investigated. The rate of change in the $O_2(^1\Delta)$ concentration in continuous-flow tube is determined by measuring the absolute spectral irradiance of the $O_2-O_2(^1\Delta)-H_2O$ gas mixture in the ranges of 600–800 nm and 1210–1330 nm. The effective rate constant of $O_2(^1\Delta)$ deactivation in all possible channels of the $O_2(^1\Delta) + O_2(^1\Delta) \rightarrow$ products reaction is found to be $(8\pm1.2)\times10^{-17}$ cm^3 s^{-1}.**

Keywords: *singlet oxygen, oxygen–iodine laser, singlet oxygen generator, the rate constant the deactivation.*

1. Introduction

Singlet oxygen $O_2(a^1\Delta)$ is an energy source for chemical oxygen–iodine laser. $O_2(a)$ is produced most efficiently in a singlet-oxygen generator (SOG) in the reaction of gaseous chlorine with alkaline solution of hydrogen peroxide. The $O_2-O_2(a)-H_2O$ gas obtained, containing residual chlorine, is transported from the SOG to the laser nozzle to be mixed with iodine vapour or iodine-containing components. When transported, the $O_2-O_2(a)-H_2O$ mixture undergoes reactions leading to $O_2(a)$ deactivation:

$$O_2(a) + O_2(a) \rightarrow O_2(b) + O_2(X), \quad (1)$$

$$O_2(a) + O_2(a) \rightarrow O_2(a) + O_2(X), \quad (2)$$

$$O_2(a) + O_2(a) \rightarrow O_2(X) + O_2(X), \quad (3)$$

$$O_2(a) + O_2(X) \rightarrow O_2(X) + O_2(X), \quad (4)$$

$$O_2(a) + M \rightarrow O_2(X) + M, \quad (5)$$

$$O_2(b) + M \rightarrow O_2(a) + M, \quad (6a)$$

$$O_2(b) + M \rightarrow O_2(X) + M, \quad (6b)$$

where $O_2(X)$ and $O_2(b)$ are oxygen molecules in the ground ($^3\Sigma$) and second electronic-excited ($^1\Sigma$) states, respectively; M are H_2O, Cl_2, or O_2 molecules. The power, chemical efficiency, and weight and size characteristics of the oxygen–iodine laser depend primarily on the total pressure and content of singlet oxygen in the $O_2-O_2(a)-H_2O$ mixture. The most critical processes (from the point of view of conserving the maximally high concentration of $O_2(a)$ molecules in the gas flow) are reactions (1)–(3). The rate constant of reaction (1) were measured only in two studies: $k_1 = 2\times10^{-17}$ cm^3 s^{-1} [1] and 2.7×10^{-17} cm^3 s^{-1} [2]. There are no experimental data in the literature on the constant rates of reactions (2) and (3). In the standard kinetic package for the active medium of the chemical oxygen–iodine laser [3] the recommended rate constants for reactions (2) and (3) are, respectively, $k_2 = 0$ and $k_3 = 1.7\times10^{-17}$ cm^3 s^{-1}. The effective rate constant of $O_2(a)$ loss in reactions (1)–(3) was determined in [4, 5] [by processing the data on the $O_2(a)$ content at the SOG output] to be $\sim10^{-16}$ cm^3 s^{-1}. Concerning the theoretical studies on estimating the constant rates for reactions (1)–(3), we should also note [6, 7]. According to [6], $k_1 \approx 10^{-16}$ cm^3 s^{-1} and $k_2, k_3 \ll k_1$. In [7] the constant k_1 was calculated to be $\sim10^{-17}$ cm^3 s^{-1}, i.e., smaller than the values reported in [1, 2]. For reaction (4) the rate constant $k_4 \approx 1.6\times10^{-18}$ cm^3 s^{-1} was obtained in many independent studies [8–13]. The following values were obtained for reaction (5): $k_{5Cl_2}(M = Cl_2) = 6\times10^{-18}$ cm^3 s^{-1} [14] and $k_{5w}(M = H_2O) = 4\times10^{-18}$ cm^3 s^{-1} [11] and 5.6×10^{-18} cm^3 s^{-1} [15]. The sum of the rate constants of reactions (6a) and (6b), $k_{6M} = k^a_{6M} + k^X_{6M}$, is known to be 6.7×10^{-12} cm^3 s^{-1} at $M = H_2O$ [16], 4.5×10^{-16} cm^3 s^{-1} ($M = Cl_2$) [17], and 4×10^{-17} cm^3 s^{-1} ($M = O_2$) [18]. Reaction (6a) regenerates one $O_2(a)$ molecule to compensate for one lost in reaction (1). According to some studies, $k^X_{6M} \approx 0$, at least for $M = H_2O$ [14] and O_2 [19].

The purpose of this study is to determine the effective rate constant of $O_2(a)$ loss in reactions (1)–(3) in $O_2-O_2(a)-H_2O$ mixture by measuring the $O_2(a)$ concentrations in the continuous-flow tube. The $O_2(a)$ and $O_2(b)$ concentrations and gas temperature are determined from the emission spectra of singlet oxygen, measured using fibre spectrometers with absolutely calibrated spectral sensitivity.

2. Experimental

A schematic of the experimental setup is shown in Fig. 1. An $O_2-O_2(a)-H_2O$ gas flow was formed by a SOG, where a pure chlorine flow interacted with jets of alkaline solution of hydrogen peroxide [20]. Then the gas flow was supplied to an optical diagnostic system (ODS). This unit was a 120-mm-long quartz tube with an inner diameter of 25 mm, containing a Teflon insert with an internal channel (height, 8 mm; cross section, 2 cm^2). A slide with the receiving end of two-channel optical cable, capable of moving along the ODS, was located at a distance of 4–10.3 cm from the ODS input. The radiation

M.V. Zagidullin, N.A. Khvatov Samara Branch of P.N. Lebedev Physics Institute, Russian Academy of Sciences, Novo-Sadovaya ul. 221, 443011 Samara, Russia; e-mail: marsel@fian.smr.ru

Received 26 May 2010
Kvantovaya Elektronika **40** (9) 800–803 (2010)
Translated by Yu.P. Sin'kov

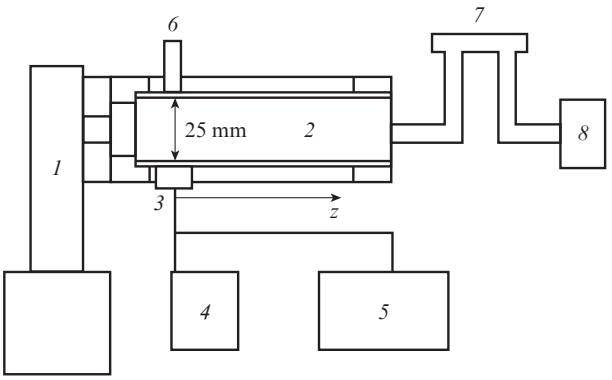

Figure 1. Schematic of the experiment:
(*1*) SOG; (*2*) optical diagnostic system (ODS); (*3*) slide with a receiving end of two-channel optical cable; (*4*) M266 spectrometer; (*5*) AvaSpec-3648 spectrometer; (*6*) Ge photodetector; (*7*) optical cell for measuring residual chlorine concentration; (*8*) backing pump.

was delivered (without optical collimators) through one of the cable channels into an AvaSpec-3648 spectrometer (Avantes, the Netherlands) with a CCD detector line. The spectrometer recorded the (0,0–0,0) and (0,0–1,0) bands of singlet oxygen dimole radiation,

$$\begin{aligned} &O_2(a,v=0) + O_2(a,v=0) \rightarrow O_2(X,v=0) \\ &\quad + O_2(X,v=0) + h\nu\ (\lambda = 634\ \text{nm}), \\ &O_2(a,v=0) + O_2(a,v=0) \rightarrow O_2(X,v=1) \\ &\quad + O_2(X,v=0) + h\nu\ (\lambda = 703\ \text{nm}), \end{aligned} \tag{7}$$

and the b–X (0–0) band (λ = 762 nm) of O_2(b) spontaneous emission in the range of 600–800 nm. The second channel of the optical cable was used to guide radiation to an M266 spectrometer (Solar, Belarus) with a photodetector line, which recorded the O_2(a) spectrum in the a–X band (λ = 1268 nm) in the range of 1210–1330 nm. The fibre–spectrometer optical system recorded radiation from molecules within a cone with an angle of 15° and a vertex located on the fibre receiving end. Approximately 80% of collected radiation was from a cone with an angle of 10° or from a gas layer 2.5 mm high, located between the ODS walls. The absolute spectral sensitivity R (in photons counts^{-1} cm^{-2} nm^{-1}) of the AvaSpec-3648 spectrometer was certified by the manufacturer with an error of 9.5% for the entire spectral range (600–800 nm). The product $R(\lambda)\delta\lambda$ (where $\delta\lambda$ is the spectral width of one line pixel) is the number of photons emitted from 1-cm^2 area of the diffuse surface of continuous radiation source in the wavelength range $(\lambda, \lambda + \delta\lambda)$ and leading to an increase in the number of counts of one CCD pixel by unity. To calibrate the absolute spectral sensitivity of the M266 spectrometer, radiation from an AvaLight-HAL tungsten lamp (Avantes) with a color temperature of 2850 K) was directed into a photometric sphere with a diffuse $BaSO_4$ coating. Radiation scattered from the sphere surface was recorded with the spectrometers in the same optical configuration as that used in the experiments. Having known the absolute sensitivity of AvaSpec-364 spectrometer, the relative spectral distribution of the lamp radiation intensity, and readings of the detector line, we determined the absolute sensitivity of the M266 spectrometer in the range of 1230–1310 nm. The error in calibrating the absolute sensitivity of M266 was estimated to be ~12%. The concentrations of $O_2(a,v=0)$ and $O_2(b,v=0)$ molecules were calculated from the formulas

$$\begin{aligned} n_a &= \frac{4}{A_a T_q L t_e} \int_{a-X} C(\lambda) R(\lambda) d\lambda, \\ n_b &= \frac{4}{A_b T_q L t_e} \int_{b-X} C(\lambda) R(\lambda) d\lambda, \end{aligned} \tag{8}$$

where $A_a = 2.19 \times 10^{-4}$ s^{-1} and $A_b = 8.8 \times 10^{-2}$ s^{-1} are the Einstein coefficients of the a–X (0–0) and b–X (0–0) transitions, respectively [21]; L = 2.5 cm is the ODS width; $T_q \approx 0.93$ is the transmittance of ODS quartz windows; t_e is the spectrum exposure time; and $C(\lambda)$ is the number of pixel counts at the wavelength λ. The integrals $4T_q^{-1}L^{-1}t_e^{-1}\int C(\lambda)R(\lambda)d\lambda$ over the spectral bands (accurate to the photon energy) are specific powers (in photons cm^{-3} s^{-1}) of radiation from a gas volume of 1 cm^3 in the corresponding spectral band. The gas temperature in the ODS was determined from the spectral width of dimole radiation (7), as in [22], with an error of ±10 K. A germanium photodetector, located at a distance of 4 cm from the ODS gas input, recorded the total radiation in the a–X oxygen band.

The deactivation frequency of excited particles of the ith type, located in a narrow gas flow layer in ODS, on a wall of rectangular channel was estimated from the formula

$$K_{ci} = \left(\frac{h^2}{8D} + \frac{2h}{\bar{u}\gamma_i} \right)^{-1}, \tag{9}$$

where γ_i is the deactivation coefficient of excited molecule on the surface, $\bar{u}$ is the average thermal velocity of particles, D is their diffusion coefficient, and h is the ODS height. Formula (9) yields the maximum estimate of the frequency (K_{cb} = 100 s^{-1}) for O_2(b) deactivation on walls under our experimental conditions for the maximum known value $\gamma_b = 10^{-2}$ [1]. Since the relative (with respect to oxygen) content of water vapour at the SOG output in this experiment was no less than 1% and the content of residual chlorine did not exceed 10%, $k_{6w}[H_2O] > 10^5$ c$^{-1} \gg (K_{cb} + k_{6O_2}[O_2] + k_{6Cl_2}[Cl_2])$, where k_{6w} is the sum of the rate constants of reactions (6a) and (6b) at M = H_2O. The equality of the production rate of $O_2(b,v=0)$ molecules in reaction (1) and their quenching rate in reaction (6) by water molecules ($k_1 n_a^2 \approx k_{6w} n_w n_b$) yields the water molecule concentration:

$$n_w = \frac{k_1}{k_{6w}} \frac{n_a^2}{n_b}, \tag{10}$$

where n_a and n_b are the concentrations of O_2(a) and O_2(b) molecules, respectively.

The chlorine concentration in the gas flow was determined with an error of 2×10^{15} cm^{-3} by measuring the absorption of nitrogen laser radiation (λ = 337 nm) in an optical cell, located after the ODS (in the flow direction), in which the gas temperature was stabilised at a level of 295 K. Gas circulation through the SOG, ODS, and optical cell was provided using a backing pump with a volume output of 5 L s^{-1}, which was constant at input gas pressures above 1 Torr. The gas pressure in the SOG, ODS, optical cell, and directly before the pump input were determined with an error of 1.5%. The measured values of the pressure; temperature; and concentrations n_w, n_a, and n_b were used to find the total oxygen concentration

n_{O_2}, the concentrations of oxygen $O_2(X)$ ($n_X = n_{O_2} - n_a - n_b$) and chlorine ($n_{Cl_2}$), the relative contents of chlorine [$F_{Cl_2} = n_{Cl_2}/(n_{Cl_2} + n_{O_2})$] and water [$F_w = n_w/(n_{Cl_2} + n_{O_2})$], and the average gas velocity in ODS.

3. Results and discussion

Few seconds after switching on the SOG, when the gas pressure in the ODS and the germanium photodetector response reached steady-state values, the slide with the receiving fibre end began to move along the ODS between the points spaced by 4 and 10.3 cm from the ODS input. The slide moved for 10 s with simultaneous scanning of singlet oxygen emission spectra. The slide position with respect to the initial point at each instant was recorded in a PC. The emission spectra in the ranges of 1210–1330 and 600–800 nm were measured each one and two seconds, respectively. The slide motion and spectral measurements lasted 10 s. Thus, we recorded ten spectra in the wavelength range of 1210–1330 nm and five spectra in the range of 600–800 nm. Some examples of the spectra recorded in one specific experiment are shown in Fig. 2. The spectra of the a–X band were used to calculate the average concentration of $O_2(a)$ molecules in each 0.63-cm-thick gas layer along the ODS. The spectra of the b–X bands and dimole radiation (7) in the gas flow in the ODS were used to find the average concentrations n_b and n_w and the gas temperature in each 1.26-cm-thick layer along the ODS.

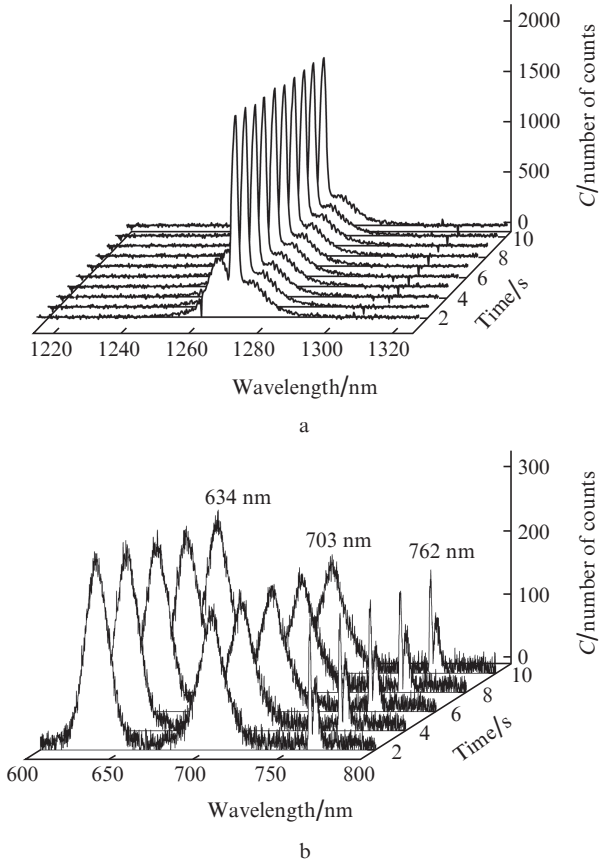

Figure 2. (a) Emission spectra in the a–X band of singlet oxygen and (b) spectra of dimole emission bands of $O_2(a)$ molecules and b–X (0–0) bands, recorded during motion of the slide with optical cable receiving end along the ODS.

A series of experiments were performed at chlorine molar flow rates of 0.3–0.5 mmol s^{-1}, gas pressures in the ODS in the range of 8–20 Torr, and average gas velocities of 120–680 cm s^{-1}. Under these conditions the relative contents of residual chlorine and water vapour at the SOG output were, respectively, $F_{Cl_2} < 4 \times 10^{-2}$ and $F_w = (2–5) \times 10^{-2}$, depending on the temperature of alkaline solution of hydrogen peroxide and the working pressure in the SOG. We did not process the data of all experiments but only those where the change in temperature along the flow did not exceed ±10 K with respect to the initial gas temperature, and the initial temperature was in the range from 340 to 390 K. The absence of significant thermal expansion (compression) of the gas flow was additionally evidenced by the constant water vapour concentration n_w along the flow during the experiment.

At $n_b \ll n_a, n_{O_2}$, relation (10) satisfied, and constant gas temperature along ODS, the change in the concentration of $O_2(a)$ molecules along the ODS (i.e., the z axis) is described by the expression

$$V\frac{dn_a}{dz} = -(k_e - k_4)n_a^2 - n_a(k_4 n_{O_2} + k_{5Cl_2} n_{Cl_2} + k_{5w} n_w + K_{ca}), \quad (11)$$

where V is the gas flow velocity and $k_e = (2 - k_{6w}^a/k_{6w})k_1 + k_2 + 2k_3$ is the effective rate constant of $O_2(a)$ quenching. Having integrated (11), we obtain

$$\frac{n_a^0}{n_a} = \left[\exp\left(\frac{K_q z}{V}\right) - 1\right]\frac{(k_e - k_4)n_a^0 + K_q}{K_q} + 1, \quad (12)$$

where $K_q = k_4 n_{O_2} + k_{5Cl_2} n_{Cl_2} + k_{5w} n_w + K_{ca}$ and n_a^0 is the $O_2(a)$ concentration at the initial slide position ($z = 0$). If $K_q z_{max}/V \ll 1$ ($z_{max} = 6.3$ cm is the maximum slide displacement along the ODS), we approximately have

$$\frac{n_a^0}{n_a} = t(k_e - k_4)n_a^0 + tK_q + 1, \quad (13)$$

where $t = z/V$ is the gas time of flight by a distance z along the ODS.

The results of measurements in each experiment were used to calculate K_q, the average concentration n_{am} of $O_2(a)$ molecules (from the spectrum recorded at the mth second), $t_m = z_m/V$, n_{a1}/n_{am} and $t_m n_{a1}$, where z_m is the slide coordinate (position) at the mth second; $m = 1–10$. The K_q values were calculated using the parameter values: $k_{5Cl_2} = 6 \times 10^{-18}$ cm^3 s^{-1} [14], $k_{5w} = 4 \times 10^{-18}$ cm^3 s^{-1} [11], $k_4 = 3.16 \times 10^{-18} \exp(-205\,K/T)$ cm^3 s^{-1} [9], $\gamma_a = 2 \times 10^{-5}$ for the $O_2(a)$ deactivation coefficient on the ODS Teflon and quartz surfaces [23, 24].

Figure 3 shows the dependence of n_{a1}/n_{am} on t_m, obtained for the experiment illustrated by Fig. 2, the parameter values being as follows: pressure in the ODS 15 Torr; concentrations $n_{a1} = 1.62 \times 10^{17}$ cm^{-3}, $n_{O_2} = 3.43 \times 10^{17}$ cm^{-3}, $n_{Cl_2} = 1.4 \times 10^{16}$ cm^{-3}, $n_w = 1.3 \times 10^{16}$ cm^{-3}; temperature $T = 390$ K; $V = 510$ cm s^{-1}; $t_{10} = z_{max}/V \approx 0.01$ s; $K_{ca} = 0.63$ s^{-1}; $k_4 n_{O_2} = 0.64$ s^{-1}; and $K_q = 1.42$ s^{-1}. Since $K_q t_{10} = 0.017$, approximation (13) can be used. A linear approximation of the dependence of n_{a1}/n_{am} on t_m yields $(k_e - k_4)n_{a1} + K_q = 14.8 \pm 0.5$ s^{-1}; hence, $k_e = (8.2 \pm 0.2) \times 10^{-17}$ cm^3 s^{-1}. Figure 4 shows the dependence of $n_{a1}/n_{am} - K_q t_m$ on $t_m n_{a1}$, obtained from the results of all the

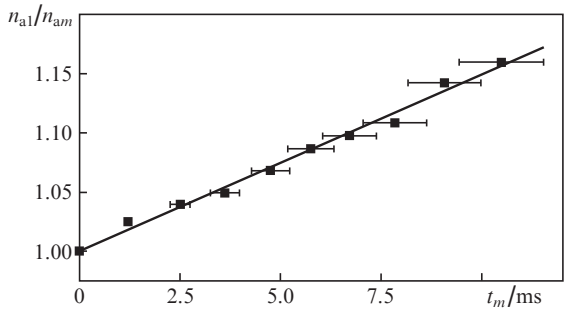

Figure 3. Change in the $O_2(a)$ concentration along the ODS.

experiments in which the initial temperature was in the range of 340–390 K. A linear approximation of this dependence yields $k_e - k_4 = (7.8\pm0.2)\times10^{-17}$ cm^3 s^{-1}. Assuming that $k_4 \approx 1.8\times10^{-18}$ cm^3 s^{-1} (T = 360 K), we find the rate constant $k_e = (8\pm0.2)\times10^{-17}$ cm^3 s^{-1}. Taking into account the errors in determining n_{a1}, flow velocity V (because of the errors in measuring the gas temperature), and the spread in the data in the literature on k_4 ($\pm10^{-19}$ cm^3 s^{-1} [8–13]) and γ_a ($\pm10^{-5}$ [23, 24]), we obtain $k_e = (8\pm1.2)\times10^{-17}$ cm^3 s^{-1}.

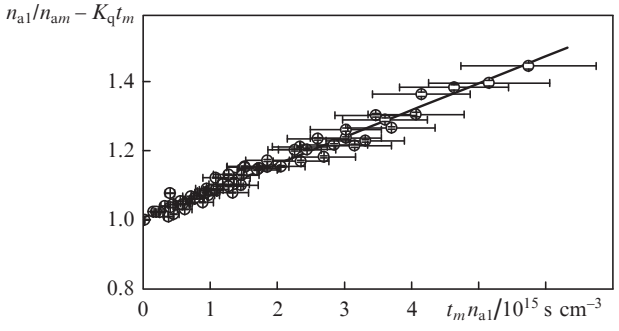

Figure 4. Change in the $O_2(a)$ concentration as a result of reactions (1)–(3).

This value of effective $O_2(a)$ self-quenching constant exceeds that given in the standard kinetic package for the active medium of a chemical oxygen–iodine laser [3] but is comparable with the rate constant obtained by processing the large data set of the SOG tests [4, 5]. According to [14, 19], $k_{6w}^{X} \ll k_{6w}^{a}$; i.e., the quenching of $O_2(b)$ by a water molecule obeys the Wigner rule [25]. Then, $k_e = k_1 + k_2 + 2k_3$. Within this study it was impossible to determine which of reactions (1)–(3) makes the main contribution to the effective rate constant k_e.

4. Conclusions

The effective rate constant of deactivation through all possible channels of reaction of the $O_2(a) + O_2(a) \rightarrow$ products type was determined from the measured concentrations of $O_2(a)$ molecules in O_2–$O_2(a)$–H_2O gas flow through a continuous-flow channel. The rate constant obtained, $(8\pm1.2)\times10^{-17}$ cm^3 s^{-1}, exceeds by a factor of 1.5 the generally accepted value, given in the standard kinetic package for an oxygen–iodine laser [3].

References

1. Derwent R.G., Thrush B.A. *Trans. Far. Soc.*, **67**, 2036 (1971).
2. Lilenfeld H.V., Carr P.A.G., Hovis F.E. *J. Chem. Phys.*, **81**, 5730 (1984).
3. Perram G.P. *Int. J. Chem. Kinet.*, **27**, 817 (1995).
4. McDermott W.E., Hobbs K., Henshaw T. *Proc. SPIE Int. Soc. Opt. Eng.*, **7131**, 713112L (2007).
5. Yang T.T., Copeland D.A., Bauer A.H., et al. *AIAA Paper* № 97-2384 (1997).
6. Liu J., Morokuma K. *J. Chem. Phys*., **123**, 204319 (2005).
7. Lu R., Zhang P., Chu T., Xie T., Han K. *J. Chem. Phys.*, **126**, 124304 (2007).
8. Wildt J., Bednarek G., Fink E.H., Wayne R.P. *Chem. Phys.*, **122**, 463 (1988).
9. Billington A.P., Borrell P. *J. Chem. Soc. Faraday Trans. 2*, **82**, 963 (1986).
10. Borrell P., Borrell P.M., Pedley D. *Chem. Phys. Lett.*, **51**, 300 (1977).
11. Schurath U. *J. Photochemistry*, **4**, 215 (1975).
12. Furui E., Akai N., Ida A., Kawai A., Shibuya K. *Chem. Phys. Lett*., **471**, 45 (2009).
13. Leiss A., Schurath U., Becker K.H., Fink E.H. *J. Photochemistry*, **8**, 211 (1978).
14. Singh J.P., Setser D.W. *J. Phys. Chem.*, **89**, 5353 (1985).
15. Findlay F.D., Snelling D.R. *J. Chem. Phys.*, **55**, 545 (1971).
16. Aviles R.G., Muller D.F., Houston P.L. *Appl. Phys. Lett.*, **37**, 358 (1980).
17. Choo K.Y., Leu M. *Int. J. Chem. Kinet.*, **17**, 1155 (1985).
18. Knickelbein M.B., Marsh K.L., Sercel J., Siebert L.D., Busch G.E. *IEEE J. Quantum Electron.*, **24**, 1278 (1988).
19. Knickelbein M.B., Marsh K.L., Ulrich O.E., Busch G.E. *J. Chem. Phys.*, **87**, 2392 (1987).
20. Azyazov V.N., Zagidullin M.V., Nikolaev V.D., Svistun M.I., Khvatov N.A. *Kvantovaya Elektron.*, **22**, 443 (1995) [*Quantum Electron*., **25**, 423 (1995)].
21. Rothman L.S., Jacquemart D., Barbe A., et al. *J. Quant. Spectr. Rad. Transfer*, **96**, 139 (2005).
22. Zagidullin M.V., Nikolaev V.D., Svistun M.I., Khvatov N.A., Fomin E.A. *Opt. Spektrosk.*, **105**, 223 (2008).
23. Ryskin M.E., Chernysh V.I., Kureneva T.Ya. *Khim. Fiz.*, **9**, 163 (1990).
24. Cranbage R.P., Dorko E.A., Johnson D.E., Whitefeld P.D. *Chem. Phys*., **169**, 267 (1993).
25. Kondrat'ev V.N. Nikitin E.E. *Kinetika i mekhanizm gazofaznykh reaktsii* (Kinetics and Mechanism of Gas-Phase Reactions) (Moscow: Nauka, 1974) p. 107.